doi.org/10.36721/PJPS.2026.39.1.REG.14186.1

Schiff-based metal complexes of atenolol: Synthesis, characterization, molecular docking and biological evaluation

Umair Ikram Dar[1,2], Kishwar Sultana[3], Saima Najm[2]*, Nadeem Ahmed[4] and Saima[2]

[1]Faculty of Pharmacy, University of Lahore, Lahore, Pakistan
[2]Faculty of Pharmacy, Lahore College of Pharmaceutical Sciences, Lahore, Pakistan
[3]Department of Pharmacy and Allied Health Sciences, Iqra University, Islamabad, Pakistan
[4]National Centre of Excellence in Molecular Biology, University of the Punjab, Lahore, Pakistan.

Abstract: **Background**: The study also emphasizes the deployment of economical synthetic methods for obtaining more potent derivatives of commercially available drugs. **Objective**: The present study aimed to synthesize schiff-base (SB) derivatives of atenolol (ATN) and their metal complexes with copper and zinc; further characterized by various spectroscopic techniques as well as biological assay. **Method**: The synthesized compounds are subjected to in-silico docking and ADME (using Swiss ADME program) studies to confirm their suitability as lead molecule. Antioxidant, antimicrobial and anticancer activities were carried out using DDPH, disk diffusion method and MTT using HepG2 cell lines respectively. Additionally; Anti-hypertensive activity was tested L-NAME induced hypertensive rat model through invasive method. **Results**: Molecular docking studies indicate higher score for 4_c and 5_e than parent drug atenolol (ATN); SB and their metal derivatives also indicate promising therapeutic profile with good GIT absorption parameters. Here 4a represents potent antioxidant activity with IC50 = 8.95 ± 11µg/ml; when compared to std. drug Ascorbic acid with an IC50= 8.3± 11µg/ml. Furthermore; all the metal complexes are reactive against *B.Subtilis* a gram +ve bacteria than gram -ve *E.Coli*, 4a (39.31mm) and 4b (42.02mm) possessed higher antimicrobial activity when compared to std. drug Vancomycin (31.48mm). The results from MTT assay reveals higher anticancer potential (%age inhibition) of 4a (73%), 4d (75%) and 5d (74%) when compared to std. drug Doxorubicin (101.2%) at HepG2 cell lines. In-vitro analysis shows significant results with SB metal derivatives, where, Zn complexes of SB derivatives (5_{a-e}) represents excellent anti-hypertensive activity in rats in contrast to standard drug alone. **Conclusion**: The imine Schiff based derivatives of atenolol and their metal complexes exhibit good biological efficacy as well as multi modal effects when compared to the frequently prescribed drug, atenolol.

Keywords: Anticancer; Anti-hypertensive; Atenolol, Molecular docking; Schiff bases

Submitted on 26-02-2025 – Revised on 20-06-2025 – Accepted on 15-07-2025

INTRODUCTION

Over the past few decades, the development of new and potent beta-blockers has represented a challenge with no significant progress (Pierin *et al.*, 2019). Adrenergic receptors consist of an integral part of autonomic nervous system responsible for various physiological processes in human body, but the risk of cardiac arrest in hypertensive (HTN) patients is two-three-fold more than in healthy individuals (Deshmukh *et al.*, 2011, Baek *et al.*, 2018). As proper blood circulation and cardiac health are crucial for human survival, management of cardiovascular disorders holds prime importance in the health-care system (Denoble, 2013). Beta-blockers refer to a group of drugs having broad pharmacokinetic and pharmacodynamic range (Wiysonge *et al.*, 2017). Despite some controversies in their use as first line therapy in certain clinical scenarios, it was declared to be the fourth most prescribed drug in the United States (Diaconu *et al.*, 2019, James *et al.*, 2014). As increased sympathetic activity a nd high catecholamine levels play a key role in pathogenesis of HTN. Blocking the adrenergic receptor, with ATN like drugs, has a profound impact in reducing blood pressure (BP) and cardiac output (Kjeldsen, 2018, Peller *et al.*, 2015). Heterocyclic compounds like pyridines, bipyridines, triazine and similar molecules represent ideal ligands due to the existence of localized electron pair with on ring nitrogen atom (Dalia *et al.*, 2018). The efficient utilization of heterocyclic compounds has led to the generation of a number of novel compounds with a variety of physical, chemical, and biologic properties, covering a wide range of stability and reactivity (Haripriya and Subash, 2020). In last few years, there has been a rapid increase in development of metal (M) complexes as chemotherapeutic agents; due to the presence of coordination site belonging to nitrogen hetero atomic ring (e.g., imidazole, pyrazine, pyridine etc.) with DNA binding properties (Kuyper and Khan, 2014). SB complexes have potential use as anticancer, antibacterial and antiviral agents as suggested by latest researches (Tabassum *et al.*, 2013). Metal complexes of SB (SB-M) have been given enough attention because of their crucial role in homogeneous and heterogeneous catalysis (Rauf *et al.*, 2020), In particular, the cobalt (II), Cu (II) and Zn (II) SB complexes are receiving much attention due to their bio-relevant, redox nature and pharmacological activities such

**Corresponding author:* e-mail: saminajm@hotmail.com

as anticancer (Li and Yan g, 2009) antioxidant and DNA/protein targeting activity (Li *et al.*, 2014). These are the condensation products of primary amines with carbonyl compounds and were initially reported by Hugo Schiff (Zhang *et al.*, 2012); comprises of azomethine or the imine (-C=N-) functional group (Boulechfar *et al.*, 2023). The nitrogen atom of imine group may interfere with typical cellular functions through formation of a hydrogen bond with primary centers of cellular constituents (Alorini *et al.*, 2022). SB's have been widely used in the production of numerous biologically and industrially active compounds like, 4-thiazolidinines, benzoxazines, formazans, and so forth, through replacement reactions, ring closure and cycloaddition (Vashi and Naik, 2004). They possess flexible protein structure intended for drug design and development pertaining to various pharmacologically active analogues (Jarrahpour *et al.*, 2007). Computational techniques provide advantage to investigate mechanisms, targeted receptors and drugs at deeper levels; especially in analysis of big-data sets and eliminate heterogeneity of available data (Khan *et al.*, 2014).

Our concern here is to develop SB of ATN (ATN-SB) by using different aldehydes and then synthesize their metal coordinates containing ions such as Zn and Cu, in order to increase affinity against different receptors. As recognizing new molecules to be used in cancer and HTN therapy is always required; so, ATN-SB metal (ATN-SBM) derivatives being antihypertensive drug are also investigated against cancer cells *in vivo* as well as to enhance their antioxidant and anti-inflammatory potential. Hence, it is a small struggle in the direction of novel drug discovery and development of antihypertensive category with anticancer and anti-inflammatory properties. All the synthesized derivatives were examined by TLC (thin layer chromatography) on precoated silica gel G-25-UV254 plates with n-hexane and ethyl acetate in a ratio of 1:1. Later, it is also used in development of safety profiles against various targets; after analyzing their pharmacokinetic and pharmacodynamic interactions at cellular level.

MATERIALS AND METHODS

Atenolol was received as a gift from Wilshire Labs, Lahore, Pakistan. Solvents and all reagents used in study were ordered from Sigma Aldrich and utilized as provided; as they are of analytical grade. All the synthesized derivatives were examined by TLC on precoated silica gel G-25-UV254 plates with n-hexane and ethyl acetate (1:1) as solvents and the spots were visualized with ultra violet (UV) light of λ=254 nm and/or $KMnO_4$ (aq.) was employed as revealing agent. Electro Thermal 9100 apparatus was utilized for determination of melting point and it was reported uncorrected. Fourier Transform near Infrared (FTIR) spectroscopy was carried out using Agilent Carry 630 FTIR spectrophotometer using range of spectral regions from 4000cm^{-1} to 400 cm^{-1}; only chosen absorption maxima (vmax) were recorded in repetency (cm^{-1}). Attenuated Total Reflectance near IR (ATR-IR) spectrometer (Bruker Germany) was used to calculate IR peaks of SBMcomplexes in region of 4000cm^{-1} to 400 cm^{-1}.With a Shimadzu spectrophotometer, ligand-metal-complex atomic absorption spectra were noted at concentration varying from 100-1000mg/L. Proton (^{1}H) nuclear magnetic resonance (NMR) spectra were recorded using dimethyl sulfoxide (DMSO) in Bruker Avance Neo-400 spectrophotometer (400MHz). Carbon (^{13}C) NMR spectra were observed on a Bruker Avance Neo-400 (100MHz) with DMSO; coupling constants (J value) were expressed in hertz (Hz); chemical shifts (δ value) were reported comparative to internal DMSO solvent and documented in parts per million (ppm).

Fisher brand 112xx Series Advanced Ultrasonic Cleaners (catalog no.FB11203) are more powerful than conventional cleaners, with wide range of adjustable parameters for lab applications including cleaning, mixing, and degassing operate at 37/80Hz at voltage of 115V with 5.75 capacity. UV-Visible spectrophotometer N6000 Plus Double Beam Spectrophotometer, 190-1100nm Wavelength Range, 1nm Spectral Bandwidth, 7 inch Color Screen. The samples were incubated in Sanfa SHP-160 Biochemical Incubator with temperature range of 0-60ºC, controlled humidity ranges from 50-95% RH, fluorine free refrigeration, liner material mirror stainless steel, liner size 500 x 400 x 800mm, volume 160L, Power 500W. Electron emission and mass spectra (EI-MS) were noted by Bruker Compass Data Analyzer 4.2 instrument. Protein's crystalline structure was acquired from Protein Data Bank (PDB). Using Chem Draw16.0 software (Perkin Elmer) 3D structures of ligands and respective metal derivatives were made as it also generates IUPAC names of synthesized compounds, following IUPAC nomenclature.

Synthesis

General procedure for the synthesis of atenolol SB

Synthetic procedures were carried out according to a previously published technique, with some minor modifications (Matar *et al.*, 2015). Different SB derivatives (3a-e) of ATN (1) were synthesized by reacting the drug (1) with acetaldehyde (a), 4-methylbenzaldehyde (b), salicylaldehyde (c), vanillin (d), and cinnamaldehyde (e) (Scheme 1). The aldehydes were added in equimolar concentrations to a solution of ATN prepared in ethanol in the presence of catalytic amounts of glacial acetic acid. The reaction mixture was allowed to stir for 8 hours and observed through TLC for completion. Precipitates from the reaction mixture were separated through filtration, recrystallized and vacuum dried. Hexanes and ethyl acetate were used for purification of compounds through column chromatography. The resultant pure compounds were obtained in high yields and subjected to spectroscopic analysis.

Procedure for the synthesis of metal complexes

1.0 mmol of metal salt [$ZnCl_2$, $Cu(CH_3COOH)_2$] and SB were dissolved in 30 ml of methanol in a round bottom flask and allowed to stir for 3 hours (Scheme 1). The precipitates were filtered and flooded with 50 mL of cold methanol. The precipitates were then dried under vacuum and used for further studies. The success of reactions was confirmed using atomic absorption spectroscopy.

(E)-N-ethylidene-2-(4-(2-hydroxy-3-(isopropylamino)propoxy)phenyl)acetamide (3a)

The compound appeared as pink powder, yield: 95%, mp 120°C; IR *v* (cm^{-1}): 3654 (-OH), 3370 (N-H), 2981 (C-C), 2254 (C-H), 1668 (C=N), 1621 (C=O), 1554 (Ar, C=C), 1393 (CH3), 1179 (-C-O); ^{1}H NMR (400 MHz, DMSO-d6) δ: 1.21 (d, *J* = 6 Hz, 6H), 1.86 (d, 3H), 3.01 (m, 2H), 3.08-3.10 (m, 3H), 3.92 (m, 2H), 4.12 (m, 1H), 5.90 (brs, 1H), 6.86 (d, *J* = 8 Hz, 2H), 7.19 (d, *J* = 8 Hz, 2H), 8.64 (s, 1H); ^{13}C NMR (100 MHz, DMSO-d6) δ: 16.1, 18.54, 19.02, 41.61, 46.87, 50.39, 65.52, 70.11, 14.88, 129.1, 130.65, 157.38, 160.3, 173.95; HRMS (ESI), *m/z*: calcd. for C16H24N2O3Na: 315.1679 [M+Na]+ ; found 315.1682.

(E)-2-(4-(2-hydroxy-3-(isopropylamino)propoxy)phenyl) -N-(4-methylbenzylidene)acetamide (3b)

The compound appeared as powder yellow in color, yield 93%, mp 112°C; IR *v* (cm^{-1}): 3658 (-OH), 3369 (N-H), 2981 (C-C), 2257 (C-H), 1667 (C=N), 1621 (C=O), 1553 (Ar, C=C), 1389 (CH3), 1175 (-C-O); ^{1}H NMR (400 MHz, DMSO-d6) δ: 1.21 (d, *J* = 6 Hz, 6H), 2.50 (s, 3H), 3.01 (m, 2), 3.10 (m, 1H), 3.15 (s, 2H), 3.92 (m, 2H), 4.12 (m, 1H), 5.90 (brs, 1H), 6.86 (d, *J* = 8 Hz, 2H), 7.01 (d, 2H), 7.18-7.20 (d, *J* = 8 Hz, 4H), 8.81 (s, 1H); ^{13}C NMR (100 MHz, DMSO-d6) δ: 17.96, 18.54, 19.02, 41.63, 46.87, 50.39, 65.52, 70.11, 114.89, 129.1, 129.84, 130.11, 130.65, 134.69, 141.64, 157.38, 166.96, 174.01; HRMS (ESI), *m/z*: calcd. for C22H28N2O3Na: 391.1992 [M+Na]+; found 391.1985.

(E)-2-(4-(2-hydroxy-3-(isopropylamino)propoxy)phenyl) -N-(2-hydroxybenzylidene) acetamide (3c)

The compound appeared as yellow powder, yield: 92%, mp 195°C; IR *v* (cm^{-1}): 3694 (-OH), 3370 (N-H), 2920 (C-C), 2258 (C-H), 1668 (C=N), 1636 (C=O), 1553 (Ar, C=C), 1383 (CH3), 1181 (-C-O); ^{1}H NMR (400 MHz, DMSO-d6) δ: 1.21 (d, *J* = 6 Hz, 6H), 3.01 (m, 2H), 3.10 (m, 1H), 3.30 (s, 2H), 3.92 (m, 2H), 4.12 (m, 1H), 5.90 (brs, 1H), 6.85 (d, *J* = 8 Hz, 2H), 7.12 (d, 2H), 7.16 (d, *J* = 8 Hz, 2H), 7.17-7.19 (m, 4H), 7.21 (d, 2H), 8.77 (s, 1H); ^{13}C NMR (100 MHz, DMSO-d6) δ: 18.54, 19.02, 41.10, 46.87, 50.39, 65.52, 70.11, 114.3, 116.49, 118.90, 128.57, 128.6, 128.63, 129.1, 130.65, 157.38, 159.4, 160.08, 173.93; HRMS (ESI), *m/z*: calcd. for C21H26N2O4Na: 393.1758 [M+Na]+ ; found 393.1755.

(E)-2-(4-(2-hydroxy-3-(isopropylamino)propoxy)phenyl) -N-(4-hydroxy-3-methoxy-benzylidene)acetamide (3d)

The compound appeared as brown crystals, yield: 96%, mp 115°C; IR *v* (cm^{-1}): 3662 (-OH), 3370 (N-H), 2973 (C-C), 2252 (C-H), 1669 (C=N), 1634 (C=O), 1503 (Ar, C=C), 1388 (CH3), 1162 (-C-O); ^{1}H NMR (400 MHz, DMSO-d6) δ: 1.21 (d, *J* = 6 Hz, 6H), 3.01 (m, 2H), 3.10 (m, 1H), 3.33 (s, 2H), 3.40 (s, 3H), 3.92 (m, 2H), 4.12 (m, 1H), 5.90 (brs, 1H), 6.82 (m, 1H), 6.85 (d, *J* = 8 Hz, 2H), 7.12 (d, *J* = 8 Hz, 2H), 7.37 (m, 1H), 7.60 (m, 1H), 8.80 (s, 1H); ^{13}C NMR (100 MHz, DMSO-d6) δ: 18.54, 19.02, 41.12, 46.87, 50.39, 65.52, 70.11, 110.3, 114.3, 115.7, 127.1, 128.5, 129.1, 130.0, 148.8, 155.9, 157.38, 162.7, 173.93; HRMS (ESI), *m/z*: calcd. for C22H28N2O5Na: 423.1890 [M+Na]+ ; found 423.1899.

2-(4-(2-hydroxy-3-(isopropylamino)propoxy)phenyl)-N-((1E,2E)-3-phenylallylidene) acetamide (3e)

The compound appeared as red powder, yield: 87%, mp 206°C; IR *v* (cm^{-1}): 3669 (-OH), 3372 (N-H), 2980 (C-C), 2255 (C-H), 1668 (C=N), 1636 (C=O), 1557 (Ar, C=C), 1394 (CH3), 1178 (-C-O); ^{1}H NMR (400 MHz, DMSO-d6) δ: 1.21 (d, *J* = 6 Hz, 6H), 3.01 (m, 2H), 3.10 (m, 1H), 3.27 (s, 2H), 3.92 (m, 2H), 4.12 (m, 1H), 5.90 (brs, 1H), 6.84 (m, 1H), 6.87 (d, *J* = 8 Hz, 2H), 7.12 (d, *J* = 8 Hz, 2H), 7.20 (d, 2H), 7.25 (d, 1H), 8.76 (s, 1H); ^{13}C NMR (100 MHz, DMSO-d6) δ: 18.54, 19.02, 41.11, 46.87, 50.39, 65.52, 70.11, 114.9, 128.64, 129.5, 130.0, 130.11, 130.65, 130.79, 134.63, 141.3, 157.38, 163.90, 173.70; HRMS (ESI), *m/z*: calcd. for C23H28N2O3Na: 403.1992 [M+Na]+ ; found 403.1987.

(E)-N-ethylidene-2-(4-(2-hydroxy-3-(isopropylamino) propoxy)phenyl)acetamide copper acetate coordinate complex (4a)

The compound appeared as crystals green in color, yield: 94%, mp 116°C; IR *v* (cm^{-1}): 1649 (C=N), 1542 (C=O); atomic absorption (mg/L): 0.24.

(E)-2-(4-(2-hydroxy-3-(isopropylamino)propoxy)phenyl) -N-(4-methylbenzylidene) acetamide copper acetate coordinate complex (4b)

The compound appeared as crystals green in color, yield: 82%, mp 208°C; IR *v* (cm^{-1}): 1644 (C=N), 1557 (C=O); atomic absorption (mg/L): 1.24.

(E)-2-(4-(2-hydroxy-3-(isopropylamino)propoxy)phenyl) -N-(2-hydroxybenzylidene) acetamide copper acetate coordinate complex (4c)

The compound appeared as green crystals, yield: 93%, mp 212°C; IR *v* (cm^{-1}): 1642 (C=N), 1552 (C=O); atomic absorption (mg/L): 0.40.

(E)-2-(4-(2-hydroxy-3-(isopropylamino)propoxy)phenyl) -N-(4-hydroxy-3-methoxy-benzylidene)acetamide copper acetate coordinate complex (4d)

The compound appeared as green crystals, yield: 85%, mp 220°C; IR *v* (cm^{-1}): 1652 (C=N), 1546 (C=O); atomic absorption (mg/L): 1.31.

2-(4-(2-hydroxy-3-(isopropylamino)propoxy)phenyl)-N-((1E,2E)-3-phenylallylidene) acetamide copper acetate coordinate complex (4e)

The compound appeared as green crystals, yield: 88%, mp 198°C; IR *v* (cm^{-1}): 1639 (C=N), 1542 (C=O); atomic absorption (mg/L): 1.45.

(E)-N-ethylidene-2-(4-(2-hydroxy-3-(isopropylamino) propoxy)phenyl)acetamide zinc chloride coordinate complex (5a)

The compound appeared as brown powder, yield: 86%, mp 215°C; IR *v* (cm^{-1}): 1646 (C=N), 1550 (C=O); atomic absorption (mg/L): 1.52.

(E)-2-(4-(2-hydroxy-3-(isopropylamino)propoxy)phenyl) -N-(4-methylbenzylidene) acetamide zinc chloride coordinate complex (5b)

The compound appeared as powder brown in color, yield: 90%, mp 210°C; IR *v* (cm^{-1}): 1642 (C=N), 1563 (C=O); atomic absorption (mg/L): 1.80.

(E)-2-(4-(2-hydroxy-3-(isopropylamino)propoxy)phenyl) -N-(2-hydroxybenzylidene) acetamide zinc chloride coordinate complex (5c)

The compound appeared as brown powder, yield: 85%, mp 198°C; IR *v* (cm^{-1}): 1649 (C=N), 1553 (C=O); atomic absorption (mg/L): 0.45.

(E)-2-(4-(2-hydroxy-3-(isopropylamino)propoxy)phenyl) -N-(4-hydroxy-3-methoxy-benzylidene)acetamide zinc chloride coordinate complex (5d)

The compound appeared as brown powder, yield: 99%, mp 220°C; IR *v* (cm^{-1}): 1659 (C=N), 1547 (C=O); atomic absorption (mg/L): 1.40.

2-(4-(2-hydroxy-3-(isopropylamino)propoxy)phenyl)-N-((1E,2E)-3-phenylallylidene) acetamide zinc chloride coordinate complex (5e)

The compound appeared as brown powder, yield: 89%, mp 205°C; IR *v* (cm^{-1}): 1693 (C=N), 1548 (C=O); atomic absorption (mg/L): 2.30

Experimental animals

200-250 g weighing male healthy adult albino rats were used for the research. The animals were obtained from the animal research facility of UOL (University of Lahore), Lahore, Pakistan. All animals were housed in different metal cages with sufficient ventilation and maintained standard conditions (20 ± 5 °C temperature; humidity 45 ± 10%; 12h light/dark cycle). Standard rodent diet and water *ad libitum* were provided to all animals.

Solubility studies

The solubility of all the resultant products was checked. For this purpose, 5 mL of solvent (w/v) was used to dissolve 5mg of each compound. The solutions were observed for clarity/turbidity. Solvents used included distilled water, ethanol, acetone, methanol, chloroform, n-hexane, ethyl acetate, DMSO, dichloromethane and diethyl ether (Jabeen *et al.*, 2018).

Docking studies

Molecular docking studies were done using Auto Dock 4.2 software. Three-dimensional (3D) crystal structure of human beta 1 adrenergic receptor was downloaded from RCSB protein data bank (PDB) with PDB ID: 7BVQ (Protein Data Bank, 2020) whereas the 2D structure of the ligands was created using ACD Chem Sketch software (for structural details see supplementary Table S1) and saved as MDL file format. Open Babel GUI was used for 3D protonation and energy minimization to PDB. Modeling of the crystal structure of 7BVQ was carried out using Auto Dock tools 1.5.6 and the impurities were eliminated with addition of partial charges and polar hydrogen. The files were stored in form of PDBQT files for the study of protein ligand interactions. After protein-ligands docking at 7BVQ receptors ten different docked conformations were achieved. From these bio-active conformations the best was selected keeping in view the least binding energy. Protein Ligand Interacting Profiler (PLIP) online software was for cluster analysis.

The docking protocols were authenticated by re-docking technique; in both cases the active site of protein was used for re-docking the co-crystallized ligands. Then RMSD (root mean square deviation) was derived and its value of <2.0Å was perceived as accurate for evaluation of binding conformation of ligands in all the cases.

ADME prediction

Swiss ADME online software was used for the determination of molecule properties, like; absorption, distribution, metabolism, elimination (ADME) and Lipinski's parameters. Drug solubility, topological polar surface area (tPSA) and blood brain barrier (BBB) permeability were also assessed (Daina *et al.*, 2017).

Toxicity studies

Following the OECD guideline (OECD-423), acute and sub-acute studies were conducted to assess the safety of newly synthesized compounds (Schlede, 2002)b; (Toxicity–Up, 2001). All the selected animals were 12 weeks old. The selected animals were marked for identification and kept in cages for 5 days for acclimatization, the period in which they were kept at standard conditions (22 °C, RH 60-70%, standard diet and water (ad libitum). Test dose was prepared at concentrations of 5, 50, 300 and 2000mg/kg body weight keeping the maximum volume of 10ml/kg under consideration. Before the administration of the test dose the animals were denied access to food and water for 4 hours and their weight was calculated and the doses were administered accordingly. A total of three rats were included in the test group whereas the second group was treated as control and was administered the vehicle only. After the administration, the animals were kept in a fasting state for one more hour. Both groups were observed for any physical and behavioral abnormalities for an initial period of 24 hours (acute) and an extended period of 14 days (sub-acute toxicity). On the basis of the mortality rate, next doses were selected and administered to another group of 3 animals. The LD50 was calculated which also helps to

establish the dose to be administered to rats for further studies. Changes in animal fur and skin, eye redness, lacrimation, skin itching, salivation, mucous membrane, urine frequency and color, somatomotor activity, unusual behavioral patterns, sleep, convulsions, tremors and respiration were also observed.

Biological screening

Antioxidant assay

The antioxidant potential of ATN SB and its Zn and Cu metal complexes was assessed by 2,2-diphenyl-1-picrylhydrazyl (DPPH) assay. Aqueous methanol (80 %) was used for the preparation of DPPH (0.2 mM), and ATN SB and its Zn and Cu metal complex solution were prepared in methanol (350 mg/ml) and serially diluted to obtain 300 mg/ml, 250 mg/ml, 200 mg/ml, 150 mg/ml and 100 mg/ml respectively. Vitamin C (Ascorbic acid) was used as a standard. The control solution was devoid of SB and its Zn and Cu metal complexes. DPPH solution (2 ml) was added to 2ml of sample, mixed, and incubated for half an hour at 37 °C in dark. At 517 nm (Anjum *et al.*, 2023), absorbance was detected using UV/Vis Spectrophotometer against a blank. For each sample the readings were taken as duplicates.

$$\%\text{RSC} = \left[\frac{\text{Absorbance of control} = \text{Absorbance of sample}}{\text{Absorbance of control}}\right] \times 100$$

The formula's control absorbance is DPPH's absorbance, whereas the absorbance value of sample is the absorbance of test sample (Aslam *et al.*, 2024). The inhibitory concentration 50 (IC_{50}) was determined by non-linear regression curve utilizing GraphPad Prism software (Butt *et al.*, 2019).

Antimicrobial assay

Using the previously explained disk diffusion method the recently synthesized SB and their respective metal complexes were investigated for antifungal and antibacterial potentials. For antibacterial assay, two strains of bacteria i.e *Bacillus subtilis (B.subtilis)* and *Escherichia coli (E.coli)* having ATCC nos 6633 and 25922, respectively, were used. 100 µg of each test compound dissolved in 20 µl DMSO was introduced into 6mm diameter bore. Diameters of zone of inhibition were measured after 24 hours. Vancomycin 100 µg was used as standard drug. Antifungal assay was carried out on clinical strains of *Candida Albicans* and *Aspergillus Niger*. Standard drug used was Amphotericin B 100 µg (Touqeer *et al.*, 2014).

Anticancer assay

Hepatocellular carcinoma cell lines (HepG2) were harvested in DMEM with 10% FBS, 1.75g $NaHCO_3$ and 1% Penicillin-Streptomycin solution using T75 cell culture flask. Hemocytometer was used to count the cells and 100µL of solution (1 x 10^5 cells) was added to each well except for H1-H4 which were used as a blank. The plate was then incubated at 5% carbon dioxide, 95% air, 37°C and 100% humidity for 24hours. When the cell fluency in each well reached >70% the exhausted media was disposed of and substituted with 100µL of fresh media, except for H9-H12, to use them as negative control. The test compounds were solubilized in 1ml of 1X PBS and sonicated for complete dissolution and homogeneity. 100µL of the given ATN-SB and its metal complexes were added to A1-A12 as given in a template. These were then 2-fold serial diluted such that each well from A to G had two times less concentration than the previous one. The plate was then kept for incubation at 100% humidity, carbon dioxide 5%, air 95% and at 37°C for 24 hours. After incubation 3-(4,5-dimethylthiazol-2-yl)-2,5-diphenyl tetrazolium bromide (MTT) solution (10µL of 5mg/mL) was added to each well. Plate was again kept in incubator for 3 hours at 3237°C in dark conditions. The mixture was aspirated after incubation and then DMSO (100µL) was added in it in order to dissolve the formazan crystals that the live cells had created. The plate was observed at 570nm and 630nm using spectrophotometer. Doxorubicin was used as standard drug for comparison of activities (Senthilraja and Kathiresan, 2015).

In vivo anti-hypertensive activity

Anti-hypertensive activity of the ATN SB and their metal complexes was tested using an invasive hypertensive model induced by L-NAME. For invasive test, a total of 120 rats were utilized, out of which half were normotensive while others were hypertensive. In order to induce HTN, the rats were given L-NAME (40 mg/Kg) through oral route for 3 weeks. Studies were carried out on L-NAME induced hypertensive rats as well as normal healthy (normotensive) rats treated with normal saline (Pauline *et al.*, 2011). Intraperitoneal injection of diazepam and ketamine 50 mg/kg was administered to rats. Adequate induction was confirmed by the loss of pedal reflex. After the induction, the rats were laid dorsally and tied to the ends of the dissection board. A constant temperature was maintained using an overhead filament lamp. The purpose of tracheostomy was to enable unhindered, unfettered breathing. The catheters were positioned in the femoral artery to measure mean arterial blood pressure using a pressure transducer and in the femoral vein for medication injection. The rats were administered with six concentrations; 0.25 mg, 0.5 mg, 1 mg, 2mg, 3mg and 5mg, respectively, of test compounds SB & ATN SB metal complexes (n=5). The catheter's functionality was maintained by using saline solution with heparin (5000 IU m/L, v/v). A mercury manometer was used to calibrate the pressure recording equipment prior to taking the arterial BP. After a 20-minute stabilization period, SBP (Systolic Blood Pressure), DBP (Diastolic Blood Pressure) and MBP (Mean Blood Pressure) were recorded using a computerized analysis software (Lab Chart, AD Instruments, Australia) and a Power Lab data-acquisition equipment (AD Instruments, Australia) (Jahan *et al.*, 2015, Chaswal *et al.*, 2012).

Statistical analysis

The mean ± standard deviation of mean was adopted to express all values. The level of statistical significance was defined as * $P < 0.05$ when contrasted with the control group. Two-way ANOVA and then Dunnett's / Tukey's multiple comparison test were employed.

RESULTS

Chemistry

The ATN-SB derivatives (3a-e) were synthesized by reacting ATN (1) with aldehydes (2a-e) in equimolar concentration (1:1) in the presence of catalytic amount of glacial acetic acid; ethanol was used as solvent where mixture was refluxed for 8 hrs at room temperature. The synthesized SB derivatives further react with copper acetate and zinc chloride [$Cu(CH_3COOH)_2$; $ZnCl_2$] in equimolar concentration. Methanol was used as solvent and reaction mixture was stirred for 3 hrs at room temperature to generate ATN-SB-M derivatives (4a-e, 5a-e) as mentioned in Scheme-1. Rf values were calculated by using TLC technique while structures were evaluated by characterization of synthesized compounds by using various spectroscopic methods like FTIR, ^1H NMR, ^{13}C NMR and EI-MS. The ATN-SB-M derivatives were further evaluated by atomic absorption spectroscopy.

Spectroscopic data

The absorption frequencies in the FTIR showed the disappearance of the characteristic amide N-H stretch signals between 3100-3400 cm^{-1} of ATN in all of the synthesized molecules suggesting the effective shift of the amide into imine. For all imine compounds, absorption around 1667-1669 cm^{-1} was specified to C=N stretching whereas for carbonyl the values ranged between 1621-1636 cm^{-1} (as mentioned in supplementary Fig. S1 to S16). A change in the absorption in C=N and C=O regions was noticed in case of metal complexes indicating the successful metal coordination with the imine ligands. Further, proton NMR signal for imine proton appears between δ 8.64-8.81 ppm whereas the signal for imine carbon was detected between δ 160-167 ppm (see supplementary Fig. S17 to S21), while, for carbon NMR the peaks originating between 160-166 ppm demonstrates the presence of imine group and 173-174 ppm represents carbonyl group (see supplementary Fig. S22 to S26). Moreover, the atomic absorption studies also confirm the presence of metal coordinates in the compounds (see supplementary Fig. S27 to S36).

Solubility

The synthesized compounds were subjected to solubility studies using various solvents. In general, the ATN-SB and ATN-SB-M derivatives were appreciably soluble in all of the solvents except for chloroform where the solubility of the compounds was from moderate to low. Table 1 gives information about the solubility of ligands and their metal complexes.

Docking studies

Molecular docking results of 7BVQ against ATN-SB-M derivatives reveal higher docking scores than the parent drug (Table 2). The binding energy of 3b was found to be the lowest (-8.94 kcal/mol) with one hydrogen bond, indicating the highest activity amongst all the SB derivatives. Furthermore, it can also be noticed that 3b binds to THR132, PRO133, ASN134, ARG135, ILE118, GLY122, ARG123, LYS214, CYS215, CYS216, ASP217, VAL360, TRP1364 l amino acid residues in the binding pocket of receptor as compared to other compounds. Among metal derivatives, 4c shows best docking score against 7BVQ with least binding energy of -10.22 Kcal/mol. Here, 4c shows one hydrogen (ASN424) and six hydrophobic interactions (TRP174, ILE235, VAL236, TRP251, CYS333, VAL423) in the binding pocket of 7BVQ as represented in fig. 1. The docking score of ATN was found to be -7.5 Kcal/mol; with one hydrogen (THR252) and three hydrophobic interactions (VAL256, PHE335, PHE403) found in the binding pocket of 7BVQ. The binding interactions of ATN are also displayed in fig. 2. The ligands fit efficiently into the binding pocket with additional space for introduction of a larger substituent on the aromatic aldehyde scaffold.

ADME

All 15 compounds were tested for absorption, distribution, metabolism and elimination (ADME) parameters using Swiss ADME online tool in order to assess their pharmacokinetic profile. In this context, properties such as molecular weight, rotatable bonds, hydrogen bonding, surface area and solubility were studied (Table 3). Additionally, the compounds were studied for BBB permeability, gastrointestinal tract (GIT) absorption and CYP enzyme inhibition for metabolic profiling. The hydrogen bonding and log P were found to be within the prescribed limits whereas tPSA values were also lower than 140 Å which implies that the compounds have excellent membrane permeability and bio-availability (Table 4) (Newby *et al.*, 2015). BBB permeability of beta blockers provides an additional advantage as the drug can bind to the adrenergic receptors in the central nervous sytem (CNS) and elicit additional therapeutic responses (Ertl *et al.*, 2000). Among the studied compounds, 9 out of 15 compounds were BBB permeable and 3c, 3d, 4c, 4d, 5c and 5d were not capable of crossing the barrier. The CYP inhibition profile is given in Table 4. In case of original imines, most of the inhibitory activity was observed in case of CYP2D6 and CYP3A4. 01A possessed no effects on any of the enzymes that resemble those of the parent drug, ATN. All the metal complexes were active against CYP3A4 only. PAINS parameter is used to detect promiscuous compounds that are capable of displaying false positive results due to high reactivity, aggregation or some other reason. Such compounds are able to bind to multiple targets and are generally unfeasible as lead compounds(Edvinsson and Tfelt-Hansen, 2008). The current study showed that there were no PAINS alerts for any of the compounds.

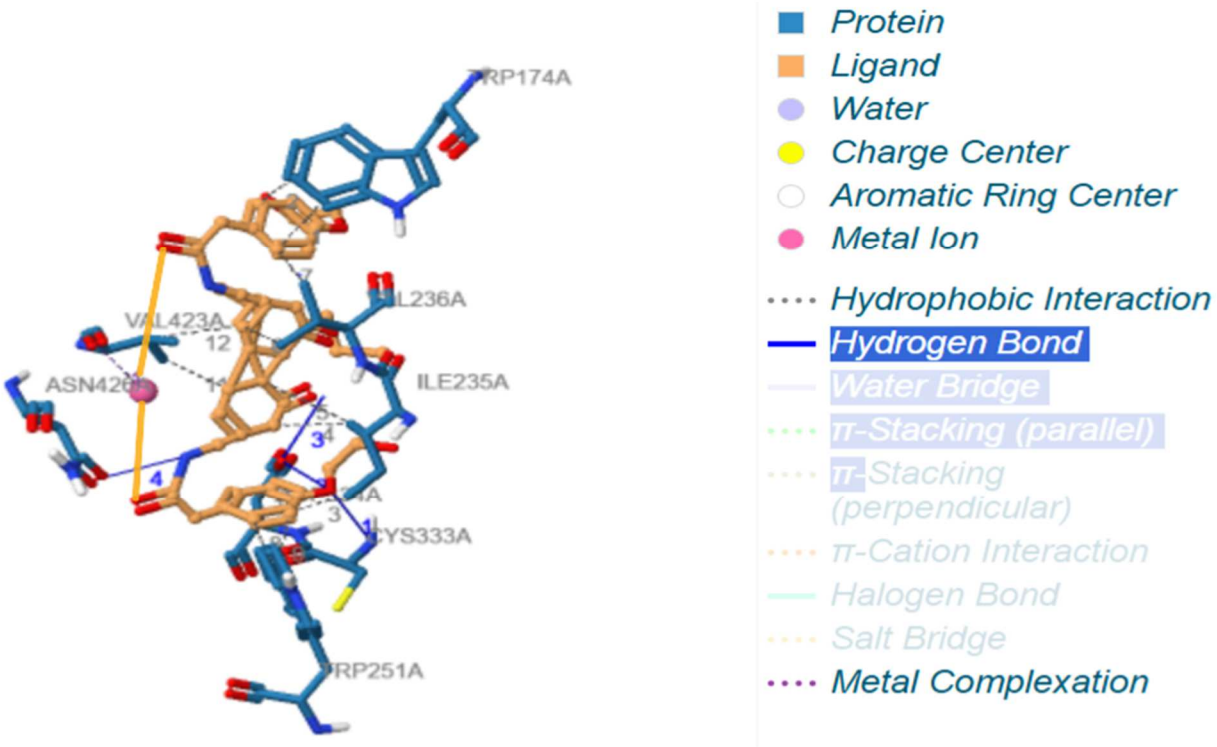

Fig. 1: Modelled 7BVQ enzyme with 4C ligand; Interacting amino acid residues shown as blue sticks with 4C ligand shown as orange sticks; in the binding pocket of 7BVQ with least binding energy of -10.22 Kcal/mol; computed by PLIP online software.

Table 1: Solubility data of compounds.

No.	Comp.	Solvents									
		Acetone	$CHCl_3$	D.W.	DCM	DMSO	Et_2O	EtOH	EtOAc	MeOH	Hexanes
1.	1	***	*	**	***	***	*	***	*	***	***
2.	3a	***	*	***	*	***	**	**	**	**	***
3.	3b	***	**	***	**	***	***	***	***	***	***
4.	3c	***	**	***	**	***	***	***	***	***	**
5.	3d	***	*	***	***	***	**	***	***	***	***
6.	3e	***	**	***	***	***	**	***	***	***	***
7.	4a	***	*	***	*	***	**	**	**	**	***
8.	4b	***	**	***	**	***	***	***	***	***	***
9.	4c	***	**	***	**	***	***	***	***	***	**
10.	4d	***	*	***	***	***	**	***	***	***	***
11.	4e	***	**	***	***	***	**	***	***	***	***
12.	5a	***	*	***	*	***	**	**	**	**	***
13.	5b	***	**	***	**	***	***	***	***	***	***
14.	5c	***	**	***	**	***	***	***	***	***	***
15.	5d	***	*	***	***	***	**	***	***	***	***
16.	5e	***	**	***	***	***	**	***	***	***	***

Solubility: completely soluble ***; sparingly soluble **; insoluble *. $CHCl_3$, chloroform; D.W, distilled water; DCM, dichloromethane; DMSO, dimethylsulfoxide; Et_2O, diethylether; EtOH, ethanol; EtOAc, ethylacetate; MeOH, methanol.

Table 2: Docking studies on atenolol, its SB ligands, along with SB-Cu and SB-Zn complexes

No	Compound	Mol. wt. (g/mol)	Docking score (Kcal/mol)	No. of H-Bonds	Interacting residues
1	1	266.33	-7.5	1	THR252, VAL256, PHE335, PHE403
2	3a	354.44	-8.67	2	THR132, PRO133, ASN134, ARG135, ARG138, GLY122, ARG123, GLU205, ARG208, CYS209, CYS215
3	3b	397.51	-8.94	1	THR132, PRO133, ASN134, ARG135, ILE118, GLY1122, ARG123, LYS214, CYS215, CYS216, ASP217, VAL360, TRP364
4	3c	370.44	-7.83	3	ASN130, PRO132, GLY122, ILE116, ARG123, TRP124, ARG206, ASP212, LYS214, CYS216, ASP217
5	3d	384.46	-8.13	1	GLN131, ILE118, GLY122, ARG123, CYS216, ASP217, PHE218, LYS214
6	3e	380.48	-7.9	1	ASN130, PRO133, LYS137, TRP157, VAL119, GLY122, ASP212, ARG206, CYS215
7	4a	353.91	-8.12	2	TRP134, PHW218, THR220, ALA225, SER228, SER229, TYR234, PHE340, ASN344, PHE359, VAL360, ASN363, TRP364
8	4b	459.04	-9.07	1	TRP134, VAL139, THR143, ASP217, PHE218, SER232, PHE340, VAL360, ASN363
9	4c	431.98	-10.22	1	TRP174, ILE235, VAL236, TRP251, CYS333, VAL423, ASN424
10	4d	462.00	-9.76	1	ASP135, VAL139, VAL142, THR143, PHE216, SER232, TRP337, PHE340, PHE341, LYS347, ARG351, PHE359
11	4e	442.01	-9.9	1	TRP134, ASP138, VAL139, VAL142, THR143, PHE216, ASP217, SER232, LYS347, ASN353, ASP351, ARG356
12	5a	355.76	-8.48	0	VAL139, THR142, GLU205, PHE218, VAL219, THR220, SER228, SER232, PHE340, PHE341, ASN344, LYS347, PHE348, ARG351
13	5b	460.90	-9.63	1	THR132, PRO133, ASN134, ARG135, ILE116, GLY122, ARG123, TRP134, LYS214, CYS216, ASP217
14	5c	433.83	-8.63	1	TRP114, GLY116, ILE118, ARG123, TRP124, LYS214, CYS215, CYS216, ASP217, ASN363, TRP364, TYR367
15	5d	463.86	-9.24	0	GLY115, ILE118, VAL119, TRP134, ASP138, VAL139, VAL142, PHE218, PHE340, TRP364, TYR367
16	5e	443.87	-10.0	1	GLN131, THR132, PRO133, ASN134, ILE118, ARG123, TRP124, TRP134, LYS214, CYS215, CYS216, ASP217

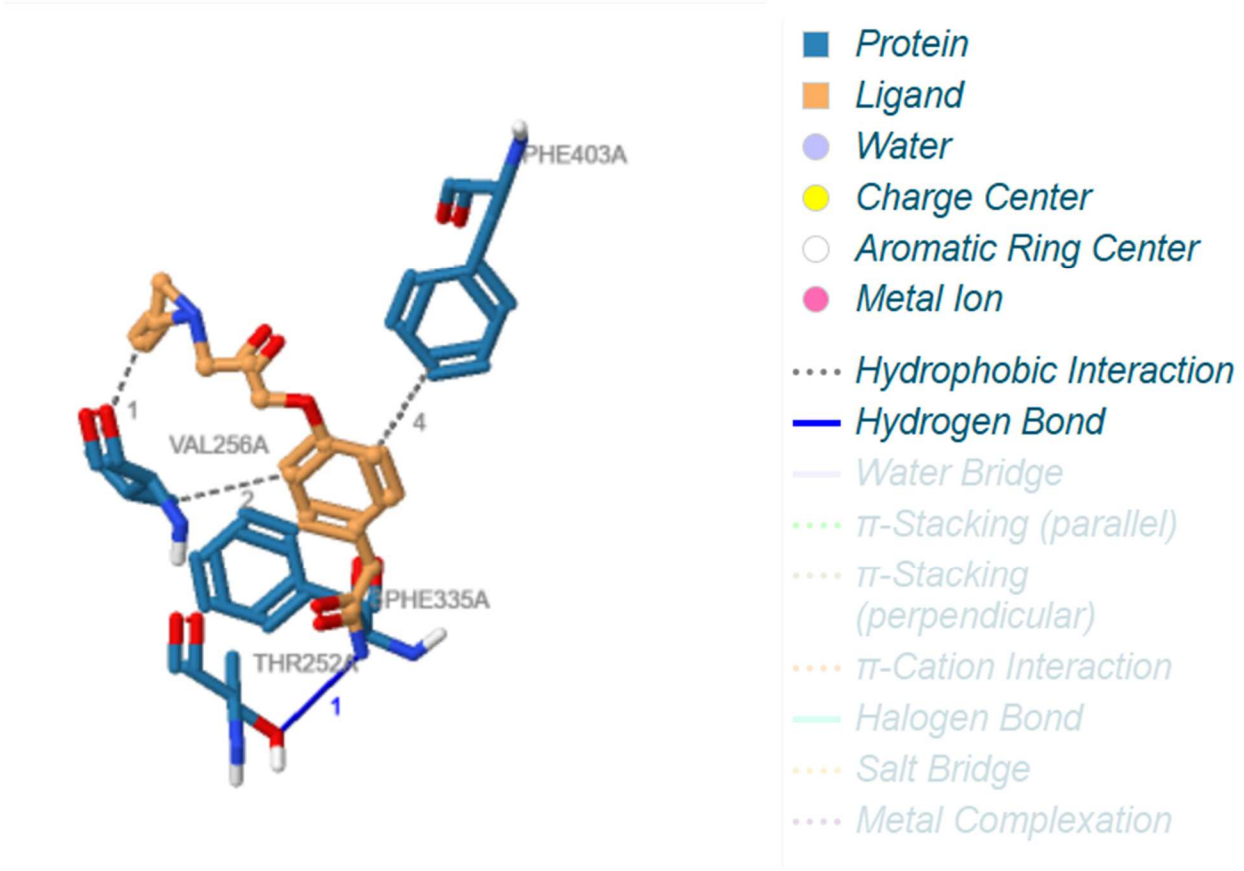

Fig. 2: Modelled ATN with 7BVQ enzyme; ATN represented as orange stick with surrounding amino acid residues represented as blue strips; modelled by PLIP online software.

Table 3: Prediction of pharmacokinetic using Swiss ADME tool.

Compound	MW	RoB	HBA	HBD	tPSA	IlogP(MlogP)	BBB	GIT	Pgp
1	266.34	8	4	3	84.58	2.17 (0.69)	No	High	No
3a	292.37	9	5	2	70.92	2.86 (1.52)	Yes	High	No
3b	397.51	11	5	2	74.16	3.67 (2.33)	Yes	High	Yes
3c	370.44	10	6	3	91.15	3.08 (190)	No	High	No
3d	400.47	11	7	3	100.4	3.51 (1.59)	No	High	Yes
3e	380.48	11	5	2	70.92	4.29 (2.80)	Yes	High	Yes
4a	426.83	9	5	2	70.92	0(2)	Yes	High	Yes
4b	502.92	10	5	2	70.92	0 (3.09)	Yes	High	Yes
4c	504.89	10	6	3	91.15	0 (2.33)	No	High	No
4d	534.92	11	7	3	100.38	0 (2.01)	No	High	No
4e	514.93	11	5	2	70.92	0 (3.22)	Yes	High	No
5a	428.66	9	5	2	70.92	0 (2)	Yes	High	Yes
5b	504.76	10	5	2	70.92	0 (3.09)	Yes	High	Yes
5c	506.73	10	6	3	91.15	0 (2.33)	No	High	No
5d	536.75	11	7	3	100.38	0(2.01)	No	High	No

Rule: molecular weight (MW) ≤500; rotatable bonds (RoB) ≤10; hydrogen bond acceptors (HBA) ≤10; hydrogen bond donors (HBD) ≤5; topological surface area (tPSA) ≤140 ´Å2; IlogP\MlogP <5.

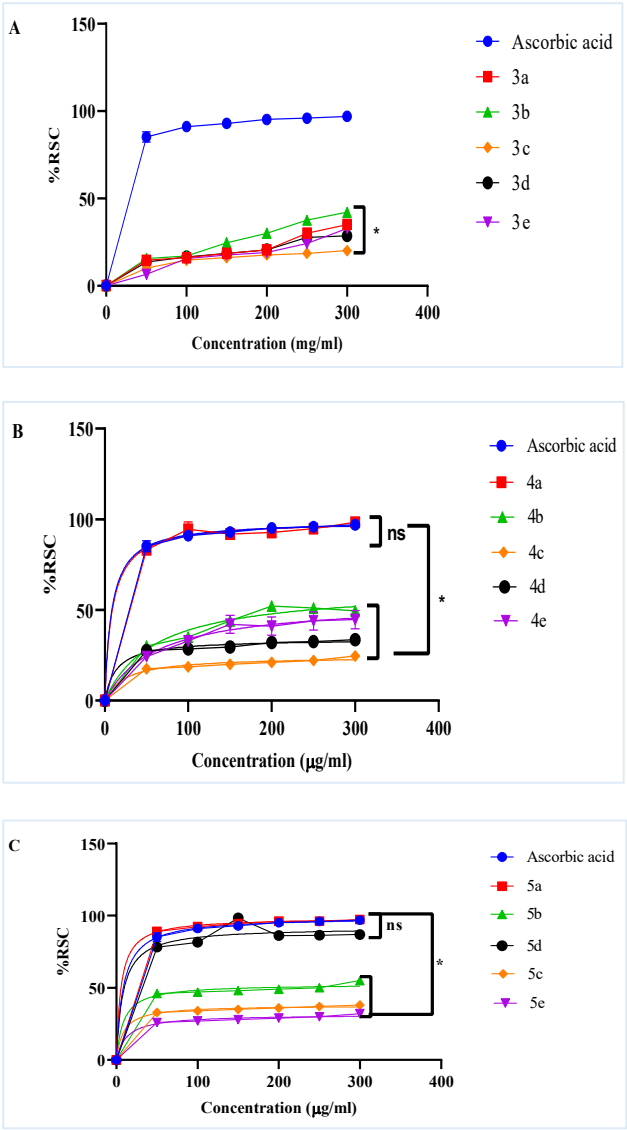

Fig. 3: Radical scavenging capacity (% RSC) of ATN SB and its copper and zinc metal complexes measured by DPPH assay. (A) % RSC of ATN SB (B) % RSC of ATN SB copper metal complexes (C) % RSC of ATN SB zinc metal complexes investigated by two way ANOVA followed by Dunnett's multiple comparison test, n=2. *P< 0.5 significant relative to Ascorbic acid whereas ns is non-significant relative to Ascorbic acid.

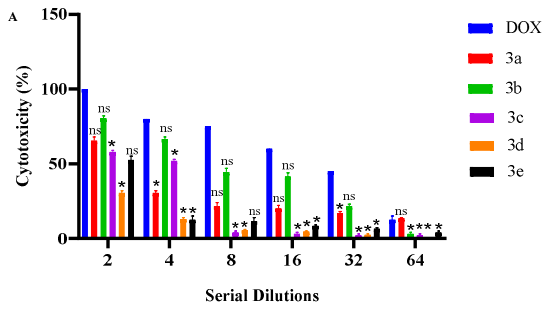

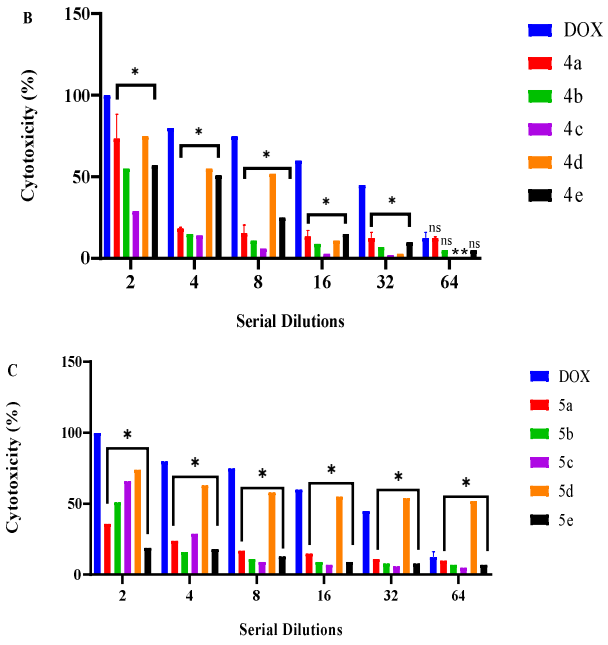

Fig. 4: MTT anticancer assay on Hepa G2 cell lines of (A) ATN SB (B) ATN SB copper metal complexes and (C) ATN SB zinc metal complexes evaluated by two-way ANOVA succeeded by Tukey's multiple comparison test, n=2.*P< 0.5 significant relative to Doxorubicin whereas ns is non-significant relative to Doxorubicin. Data has been presented as mean ± SEM.

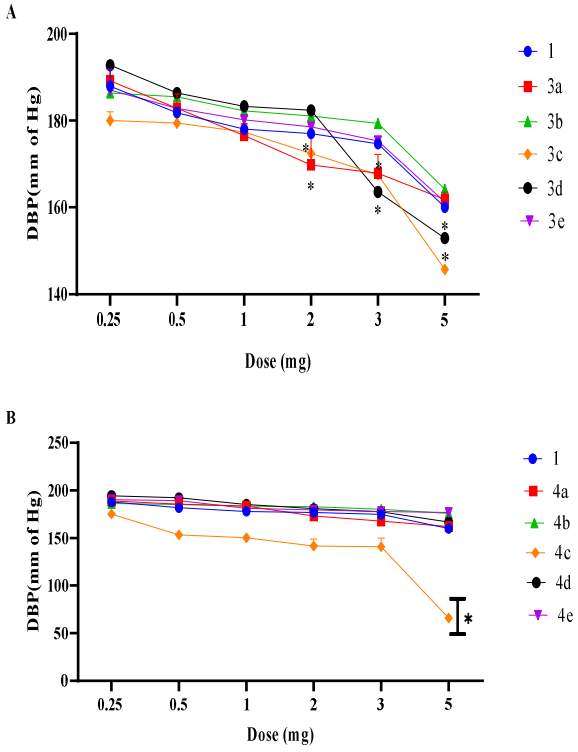

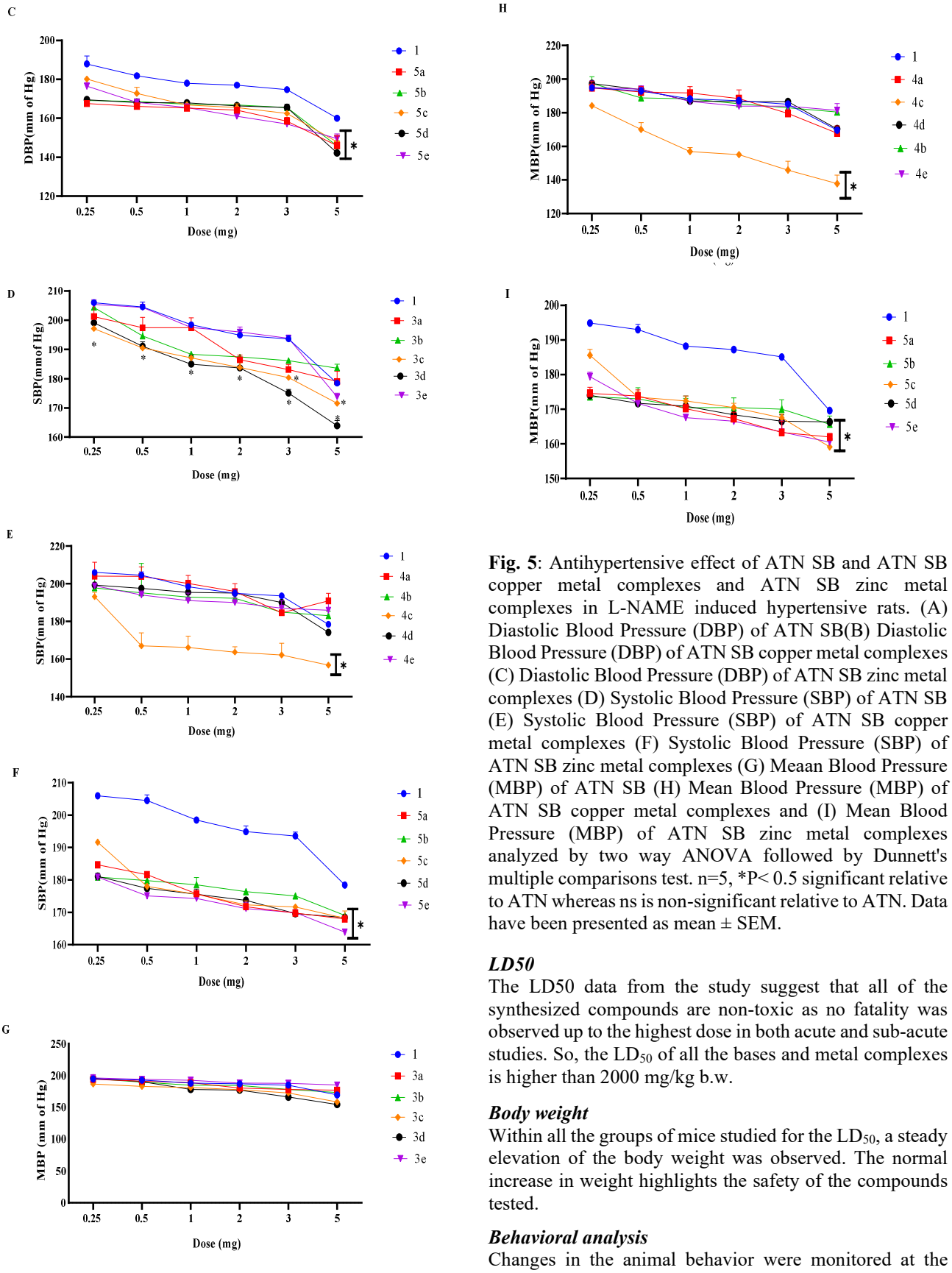

Fig. 5: Antihypertensive effect of ATN SB and ATN SB copper metal complexes and ATN SB zinc metal complexes in L-NAME induced hypertensive rats. (A) Diastolic Blood Pressure (DBP) of ATN SB(B) Diastolic Blood Pressure (DBP) of ATN SB copper metal complexes (C) Diastolic Blood Pressure (DBP) of ATN SB zinc metal complexes (D) Systolic Blood Pressure (SBP) of ATN SB (E) Systolic Blood Pressure (SBP) of ATN SB copper metal complexes (F) Systolic Blood Pressure (SBP) of ATN SB zinc metal complexes (G) Meaan Blood Pressure (MBP) of ATN SB (H) Mean Blood Pressure (MBP) of ATN SB copper metal complexes and (I) Mean Blood Pressure (MBP) of ATN SB zinc metal complexes analyzed by two way ANOVA followed by Dunnett's multiple comparisons test. n=5, *P< 0.5 significant relative to ATN whereas ns is non-significant relative to ATN. Data have been presented as mean ± SEM.

LD50

The LD50 data from the study suggest that all of the synthesized compounds are non-toxic as no fatality was observed up to the highest dose in both acute and sub-acute studies. So, the LD_{50} of all the bases and metal complexes is higher than 2000 mg/kg b.w.

Body weight

Within all the groups of mice studied for the LD_{50}, a steady elevation of the body weight was observed. The normal increase in weight highlights the safety of the compounds tested.

Behavioral analysis

Changes in the animal behavior were monitored at the intervals of 30 min, 4 h, 24 h, 7 days and 14 days. All

Table 4: Prediction of CYP inhibition using swiss ADME tool

Compound	CYP1A2 inhibition	CYP2C19 inhibition	CYP2C9 inhibition	CYP2D6 Inhibition	CYP3A4 inhibition
1	No	No	No	No	No
3a	No	No	No	No	No
3b	No	No	No	Yes	Yes
3c	No	No	No	Yes	Yes
3d	No	No	No	Yes	Yes
3e	Yes	No	No	Yes	Yes
4a	No	No	No	No	Yes
4b	No	No	No	No	Yes
4c	No	No	No	No	Yes
4d	No	No	No	No	Yes
4e	No	No	No	No	Yes
5a	No	No	No	No	Yes
5b	No	No	No	No	Yes
5c	No	No	No	No	Yes
5d	No	No	No	No	Yes
5e	No	No	No	No	Yes

physical features and behavioral patterns were found to be normal during the entire course of study.

Biological evaluation

Antioxidant activity

The % radical scavenging activity (% RSC) of ascorbic acid has been 96.91%. The % RSC of SB 3a-e had 35%, 42%, 20%, 28% and 32% respectively as shown in fig. 3a. The Cu metal complexes 4a had comparable RSC of 98% whereas, 4b-e presented less antioxidant potential relative to ascorbic acid as shown in fig. 3B. The Zn metal complexes 5a and 5d had 98% and 86% RSC similar to ascorbic acid while the 5b, 5c and 5e possessed lesser antioxidant potential relative to ascorbic acid as shown in fig. 3C. IC50 values were calculated from the DPPH data by graphical method using GraphPad Prism. The standard drug, ascorbic acid had an IC50 of 8.3±11 µg/ml, whereas the SB 3a-e had an IC_{50} of 14.9±11 µg/ml, 14.4±11 µg/ml, 6.71±11 µg/ml, 7.46±11 µg/ml and 4.73±11 µg/ml, respectively. The Cu complexes 4a-e displayed an IC50 of 8.95±11 µg/ml, 60.97±11 µg/ml 24.29 ± 11 µg/ml, 13.91 ± 11 µg/ml and 60.95±11 µg/ml respectively. The IC50 of Zn complexes 5a-e were recorded to be 5.55±11 µg/ml, 8.73±11 µg/ml, 8.65±11 µg/ml, 8.13±11 µg/ml and 12.58 ± 11 µg/ml respectively. The assay clearly highlights the high antioxidant potential of the compounds synthesized. The SBs 3c, 3d and 3e were found to be more potent than the standard compound whereas the Cu complex 4a possessed a comparable activity to the ascorbic acid. All of the Zn complexes demonstrated a high antioxidant profile with statistically significant results with only 5e showing slightly lower results than the rest of the Zn family. The antioxidant potential of compounds as radical scavenging activity is shown in fig. 3.

Antimicrobial activity

The imine derivatives and their respective complexes with metal were studied using Gram +ve *B. subtilis* and Gram -ve *E. coli.* The imines 3a-e were inactive against both bacterial strains. All the metal complexes were reactive against *B. subtilis* and possessed significant activities whereas for *E. coli*, no activity was observed (Arzumanian *et al.*, 2021). The Cu complexes, 4a and 4b possessed the highest antibacterial activity (39.31 mm and 42.02 mm) surpassing that of the standard drug (31.48 mm). No anti-fungal activity was found to be present in any of the compounds tested. The results from antibacterial activity are given in Table 5.

Table 5: Antibacterial potential of metal complexes (zones of inhibition mm).

No.	Compound	*B.Subtilis*	*E. Coli*
1.	4a	39.31 mm	Nil
2.	4b	42.02 mm	Nil
3.	4c	24.53 mm	Nil
4.	4d	23.95 mm	Nil
5.	4e	29.06 mm	Nil
6.	5a	22.56 mm	Nil
7.	5b	30.97 mm	Nil
8.	5c	23.45 mm	Nil
9.	5d	24.53 mm	Nil
10.	5e	24.01 mm	Nil
11.	Vancomycin	31.48 mm	Nil

Anticancer activity

The results from MTT assay suggested that compounds 3a (65%) and 3b (80%) possess substantial anticancer activity at multiple dilution levels (Fig. 4A).

High activity was also noticed in 3b as compared to the standard doxorubicin. Similarly, anticancer effect was also observed in the metal complex series 4 and 5 especially 4a (73%), 4d (75%) and 5d (74%) when compared to the standard drug as illustrated in fig. 4B and C. HepG2 cell lines are among the popular models for the study of

anticancer activity and drug metabolism. It accounts for 76% of all hepatic cell lines used due to its ease of use and reproducibility (Arzumanian *et al.*, 2021, Daina *et al.*, 2017).

Anti-hypertensive activity

The effect of all newly synthesized products on the blood pressure of normotensive and hypertensive rats was studied. It was noticed that the test compounds induced no effect on normotensive rats and their blood pressure remained stable during the course of study. Stress remained a major cause of HTN. Stress induces the production of endothelial nitric oxide synthase (eNOS). Animals were kept in a stress-free environment that did not generate eNOS and hence no fluctuations in BP in normotensive group relative to diseased (Ayada *et al.*, 2015). The present research suggested in case of hypertensive model, a significant decrease in SBP was recorded in all of SB except for 3e. The highest reduction was noted in case of 3d in a dose related manner. DBP lowering effect was also observed in compounds up to a significant level except for 3b and 3e which displayed a relatively lower effect as compared to the standard drug ATN. Compounds 3c and 3d were found to be most potent lowering the DBP to 145.9 mmHg and 152.4 mmHg respectively as shown in fig. 5D. The MBP was found to be comparable to standard drug (Fig. 5G).

The Cu complexes of the SB displayed similar activity as compared to ATN, except for 4c, which demonstrated to be extremely potent in lowering the systolic and diastolic blood pressure (Fig. 5B & 5E). The compounds 5a-e (zinc complexes) were observed to be most potent in case of SBP and to significant level in case of DBP (Fig. 5F & 5C). Furthermore, it was observed that all Zn complexes showed similar activity levels within their group.

DISCUSSION

The stretching and bending frequencies in the FTIR showed the disappearance of the characteristic amide (N-H) stretch signaling between 3100-3400 cm^{-1} for ATN, here all of the synthesized molecules suggesting the effective shift of the amide into imine (Alorini *et al.,* 2022). The absorption around 1667-1669 cm^{-1} was specified to C=N stretching frequencies for carbonyl, values ranged between 1621-1636 cm^{-1} (as mentioned in supplementary Fig. S1 to S16).

The change in absorption frequencies for C=N and C=O regions was noticed in metal complexes indicating the successful metal coordination with the imine ligands and the participation of both groups in the metal coordination. For ^{1}H-NMR, the absorption frequencies originating at δ 8.64-8.81 ppm represents imine proton (see supplementary Fig. S17 to S21). Moreover, those originating between 160-167 ppm represents imine in ^{13}C-NMR analysis (see supplementary Fig. S22 to S26). Furthermore, the atomic absorption studies also confirm the presence of coordinated metal in the compounds (see supplementary Fig. S27 to S36). The synthesized compounds were subjected to solubility studies using various solvents. In general, the ATN-SB and ATN-SB-M derivatives were appreciably soluble in all of the solvents except for chloroform where the solubility of the compounds was from moderate to low.

The ATN-SB and SB-M derivatives were subjected to docking studies at human β-1 adrenergic receptor (7BVQ). The docking studies on Zn and Cu complexes show higher binding affinities not only compared to ATN but in many instances higher than the uncoordinated versions of metal derivatives (Table 2). The docking scores for 5e, 5b and 5d were higher than 3b, being -10.0, -9.63 and -9.24 kcal/mol respectively. The higher score may be attributed to binding interactions with additional amino acids. It was obvious from the computational studies that the metal complexes bind to the receptor in a mono-ligand form (only one ligand molecule coordinated with metal) as a bi-ligand system would be too large to fit in the pocket of the protein.

Here the reduction in the number of hydrogen bonds being formed (e.g., from 3c to 5c) was observed. This reduction was caused by the binding of the metal at one of the prime acceptors sites (carbonyl) of the molecule. Nevertheless, the cost of this reduction is significantly counterbalanced by the introduction of two additional metal-halogen binding groups (Haripriya and Sobash, 2020). Coupling with Cu resulted in even higher docking scores as compared to Zn with four of the compounds having scores above -9.0 Kcal/mol and a maximum of -10.22 kcal/mol (4c) impressively higher than that of the parent drug 1 (-7.5 kcal/mol).

The ATN and its SB-M derivatives were tested for SwisADME properties; this helps to understand the behavior of drugs inside the body and to predict drug likeness for optimum therapeutic effects (Chaswal *et al.*, 2012). The best fit example is propranolol seen to treat migraine patients with BBB permeability (Ertl *et al.*, 2000). Among the studied compounds, 9 out of 15 compounds were BBB permeable and 3c, 3d, 4c, 4d, 5c and 5d were not capable of crossing the barrier. The CYP inhibition profile is given in Table 4.

The imines posseses most of the inhibitory activity with CYP2D6 and CYP3A4. 01A possessed no effects on any of the enzymes that resemble those of the parent drug, ATN. All the metal complexes were active against CYP3A4 only. They binds to multiple targets and generally impracticable as lead compounds (Edvinsson and Tfelt-Hansen, 2008). There were no PAIN alerts were seen in this study, the LD50 data from the study suggest non-toxic behavior of mice with no death was observed up to the highest dose in both acute and sub-acute studies. So, the LD_{50} of all the bases and metal complexes is higher than 2000 mg/kg body

weight. The normal increase in weight highlights the safety of the compounds tested. Changes in the animal behavior were monitored at the intervals of 30 min, 4 h, 24 h, 7 days and 14 days. All physical features and behavioral patterns were found to be normal during the entire course of study. Later on, the synthesized derivatives were tested for various biological activities. Firstly; antioxidant potential was evaluated by calculating IC50 values from DPPH data by graphical method using GraphPad Prism. The standard drug, ascorbic acid had an IC50 of 8.3 ± 11 µg/ml, whereas the SB (3a-e) had an IC50 of 14.9 ± 11 µg/ml, 14.4 ± 11 µg/ml, 6.71 ± 11 µg/ml, 7.46 ± 11 µg/ml and 4.73 ± 11 µg/ml, respectively. The Cu complexes 4a-e displayed an IC50 of 8.95 ± 11 µg/ml, 60.97 ± 11 µg/ml 24.29 ± 11 µg/ml, 13.91 ± 11 µg/ml and 60.95 ± 11 µg/ml respectively. The IC50 of Zn complexes 5a-e were recorded to be 5.55 ± 11 µg/ml, 8.73 ± 11 µg/ml, 8.65 ± 11 µg/ml, 8.13 ± 11 µg/ml and 12.58 ± 11 µg/ml respectively. The assay clearly highlights the high antioxidant potential of the compounds synthesized. The derivative 3c, 3d, 3e, and 4a were found to be more potent than the standard drug. All of the Zn complexes demonstrated a high antioxidant profile with statistically significant results except 5e showing slightly lower. The antioxidant potential of compounds as radical scavenging activity is shown in fig. 3. Then, these compounds were subjected to antimicrobial evaluation.

All the metal complexes were reactive against *B. subtilis* whereas no activity was observed for *E. coli*. Gram +ve and gram -ve bacteria are structurally different, they offer different sites of action for antimicrobial activity. The strong interaction between the metal and the imine moieties may be the cause of metal complexes decreased antibacterial activity (Arzumanian *et al.*, 2021). The copper complexes, 4a and 4b possessed the highest antibacterial activity (39.31 mm and 42.02 mm) surpassing that of the standard drug (31.48 mm). No anti-fungal activity was found to be present in any of the compounds tested. The results from antibacterial activity were given in Table 5.

Later on; the synthetic derivatives were subjected to anticancer activity. HepG2 cell lines are among the popular models for the study of anticancer activity and drug metabolism. It accounts for 76% of all hepatic cell lines used due to its ease of use and reproducibility (Arzumanian *et al.*, 2021, Daina *et al.*, 2017). High anticancer activity was noticed in 3b in comparison to Doxorubicin as shown in fig. 4. Lastly, the ATN-SB-M derivatives were tested in normotensive and hypertensive rat models for anti-hypertensive activity. ATN is a β blocker utilized as first line of therapy for hypertension treatment although data suggested its ineffectiveness in elderly.

It is incapable to lower cardiovascular related morbidity in geriatrics. That creates a space for the development of efficient derivatives (Tobriya, 2014). This can be considered as a positive feature of the compounds as they lack the risk of inducing hypotension and associated adverse effects. The present study demonstrates a significant decrease in SBP and DBP in all ATN-SB-M derivatives as shown in fig. 5.

CONCLUSION

The ever-growing burden on the health-care system due to higher number of cardiac patients continues and demands for drugs with improved efficacy and lower adverse effects. As such drugs are generally consumed for chronic ailments, reduction of oxidative stress can prove to be very beneficial in terms of sustaining vascular integrity and several other biochemical pathways and consequently, the physiological functions. The present study represents the broad application of the synthesized SB-M coordinates of ATN which not only possess the main anti-hypertensive activity up to a high level but also display additional advantages in terms of antioxidant, anti-microbial and anticancer studies. Molecular docking studies indicate higher score for 4_c and 5_e than parent drug atenolol (ATN); SB and their metal derivatives also indicate promising therapeutic profile with good GIT absorption parameters. Here, 4a represents good anticancer, antioxidant and antibacterial potential when compared to standard drugs; whereas 5_{a-e} represents excellent anti-hypertensive potential when compared to ATN. The high potency along with good pharmacokinetic profile and no toxicity at high doses, makes the compounds ideal candidates for further drug discovery process.

Acknowledgement
We want to convey our deepest acknowledgement to the administration of the University of Lahore and LCPS, Pakistan, for their support throughout the research work.

Authors' contributions
Conceptualization: K.S.
Data curation: U.I.D.
Formal analysis: U.I.D., N.A., S.N., S.
Investigation: U.I.D., N.A., S.
Methodology: K.S.
Project administration: K.S., S.N.
Supervision: K.S., S.N.
Writing–original draft: S.N., K.S., U.I.D.
Writing–review & editing: S.N., K.S., U.I.D.

Funding
There was no funding.

Data availability statement
All data generated or analyzed during this study are included in this published article and its supplementary information files.

Ethical approval
All research methodologies approved by the "Institutional Animal Ethics Committee" with reference No. IAEC/UOL/2019/37 in accordance with the guidelines given by the National Research Council (1996).

Conflict of interest

The authors declare no competing financial interest or personal relationship influencing publication of the work reported in this manuscript.

Supplementary data

https://www.pjps.pk/uploads/2025/12/SUP1765002680.pdf

REFERENCES

Alorini TA, Al-Hakimi AN, Saeed SES, Alhamzi EHL and Albadri AE (2022). Synthesis, characterization and anticancer activity of some metal complexes with a new Schiff base ligand. *Arab. Chem.,* **15**(2): 103559.

Arzumanian, VA, Kiseleva, OI and Poverennaya, EV. (2021). The curious case of the HepG2 cell line: 40 years of expertise. *Int. J. Mol. Str.,* **22**(23): 13135.

Aslam MI, Touqeer S, Jamil Q, Masood MI, Sarfraz A, Khan SY and Aslam F (2024). *Cenchrus ciliaris* L. ameliorates cigarette-smoke induced acute lung injury by reducing inflammation and oxidative stress. *S. Afr. J. Bot.,* **171**: 216-227.

Ayada C, Turgut G, Turgut S and Guclu Z (2015). The effect of chronic peripheral nesfatin-1 application on blood pressure in normal and chronic restraint stressed rats: Related with circulating level of blood pressure regulators. *Gen. Physiol. Biophys.,* **34**(1): 81-8.

Baek H, Cho M, Kim S, Hwang H, Song M and Yoo S (2018). Analysis of length of hospital stay using electronic health records: A statistical and data mining approach. *PloS one,* **13**(4): e0195901.

Boulechfar C, Ferkous H, Delimi A, Djedouani A, Kahlouche A, Boublia A and Benguerba Y (2023). Schiff bases and their metal complexes: A review on the history, synthesis and applications. *Inorg. Chem. Commun.*, **150**(1): 110451.

Butt, AS, Nisar, N, Mughal, TA, Ghani, N, and Altaf, I. (2019). Anti-oxidative and anti-proliferative activities of extracted phytochemical compound thymoquinone. *J. Pak. Med. Assoc.,* **69**(10): 1479.

Chaswal, M, Das, S, Prasad, J, Katyal, A, Mishra, AK, and Fahim, M. (2012). Effect of losartan, an angiotensin II type 1 receptor antagonist on cardiac autonomic functions of rats during acute and chronic inhibition of nitric oxide synthesis. *Physiol. Res.,* **61**(2): 135-44.

Daina A, Michielin O and Zoete V (2017). SwissADME: A free web tool to evaluate pharmacokinetics, drug-likeness and medicinal chemistry friendliness of small molecules. *Sci. Rep.,* **7**(1): 42717.

Dalia SA, Afsan F, Hossain MS, Khan MN, Zakaria C, Zahan ME and Ali M (2018). A short review on chemistry of schiff base metal complexes and their catalytic application. *Int. J. Chem. Stud.,* **6**(3): 2859-2867.

Denoble PJ (2013). Hypertension, left ventricular hypertrophy and sudden cardiac death in scuba diving. *Wound Care Hyperb. Med.,* **4**(3): 21-26.

Deshmukh A, Kumar G, Kumar N, Nanchal R, Gobal F, Sakhuja A and Mehta JL (2011). Effect of joint national committee VII report on hospitalizations for hypertensive emergencies in the United States. *Am. J. Cardiol.,* **108**(9): 1277-1282.

Diaconu CC, Marcu DR, Bratu OG, Stanescu AMA, Gheorghe G, Hlescu AA and Manea M. (2019). Beta-blockers in cardiovascular therapy: A review. *J.M.M.S.,* **6**(2): 216-223.

Edvinsson L and Tfelt-Hansen P (2008). The blood-brain barrier in migraine treatment. *Cephal.,* **28**(12): 1245-1258.

Ertl P, Rohde B and Selzer P (2000). Fast calculation of molecular polar surface area as a sum of fragment-based contributions and its application to the prediction of drug transport properties. *J. Med. Chem.,* **43**(20): 3714-3717.

Haripriya S and Subash K (2020). Computational screening and in silico docking analysis of non-selective beta-blockers over beta-3 adrenergic receptors. *N. J. P. P. P.,* **10**(03).

Jabeen, M, Ahmad, S, Shahid, K, Sadiq, A, and Rashid, U. (2018). Ursolic acid hydrazide based organometallic complexes: Synthesis, characterization, antibacterial, antioxidant and docking studies. *Front. Chem.,* **6**: 55.

Jahan K, Mahmood D and Fahim M (2015). Effects of methanol in blood pressure and heart rate in the rat. *J. Pharm. Bioallied Sci.,* **7**(1): 60-64.

James PA, Oparil S, Carter BL, Cushman WC, Dennison-Himmelfarb C, Handler J and Ogedegbe O (2014). Evidence-based guideline for the management of high blood pressure in adults: Report from the panel members appointed to the Eighth Joint National Committee (JNC 8). *Jama,* **311**(5): 507-520.

Jarrahpour A, Khalili D, De-Clercq E, Salmi C and Brunel JM (2007). Synthesis, antibacterial, antifungal and antiviral activity evaluation of some new bis-Schiff bases of isatin and their derivatives. *Molecules*, **12**(8): 1720-1730.

Khan M, Akhtar S and Shahid K (2014). Synthesis, characterization and *in-vitro* biological assays of triphenyltin derivatives of phenyl hydrazones. *Int. J. Pharm. Sci.,* **28**: 147-151.

Kjeldsen SE (2018). Hypertension and cardiovascular risk: General aspects. *Pharmacol. Res.,* **129**: 95-99.

Kuyper LM and Khan NA (2014). Atenolol vs nonatenolol β-blockers for the treatment of hypertension: A meta-analysis. *Can. J.Cardiol.,* **30**(5): S47-S53.

Li P, Niu MF, Niu MJ and Hong M (2014). Effect of structure and composition of copper and cobalt complexes with schiff base ligands on their DNA/protein interaction and cytotoxicity. *Z. Inorg. Allg. Chem.,* **640**(11): 2238-2246.

Li Y and Yang ZY (2009). DNA binding affinity and antioxidative activity of copper (II) and zinc (II) complexes with a novel hesperetin Schiff base ligand. *Inorg. Chem. Acta.,* **362**(13): 4823-4831.

Matar SA, Talib WH, Mustafa MS, Mubarak MS and AlDamen MA (2015). Synthesis, characterization, and antimicrobial activity of Schiff bases derived from benzaldehydes and 3, 3′-diaminodipropylamine. *Arab. Chem.,* **8**(6): 850-857.

Newby D, Freitas AA and Ghafourian T (2015). Decision trees to characterise the roles of permeability and solubility on the prediction of oral absorption. *Eur. J. Med. Chem.,* **90**: 751-765.

Pauline M, Avadhany ST and Maruthy K (2011). Non invasive measurement of systolic blood pressure in rats: A simple technique. *Al Ameen J. Med. Sci.,* **4**(4): 365-369.

Peller M, Ozieranski K, Balsam P, Grabowski M, Filipiak KJ and Opolski G (2015). Influence of beta-blockers on endothelial function: A meta-analysis of randomized controlled trials. *Cardiol. J.,* **22**(6): 708-716.

Pierin AMG, Florido CF and Santos Jd (2019). Hypertensive crisis: Clinical characteristics of patients with hypertensive urgency, emergency and pseudocrisis at a public emergency department. *Einstein (Sao Paulo),* **17**(4): eAO4685.

Rauf A, Shah A, Munawar KS, Ali S, Tahir MN, Javed M and Khan AM (2020). Synthesis, physicochemical elucidation, biological screening and molecular docking studies of a Schiff base and its metal (II) complexes. *Arab. J. Chem.,* **13**(1): 1130-1141.

Schlede E (2002). Oral acute toxic class method: OECD Test Guideline 423. *Rapporti istisan,* **41**: 32-36.

Senthilraja P and Kathiresan K (2015). *In-vitro* cytotoxicity MTT assay in Vero, HepG2 and MCF-7 cell lines study of Marine Yeast. *J. Appl. Pharm. Sci.,* **5**(3): 080-084.

Tabassum S, Amir S, Arjmand F, Pettinari C, Marchetti F, Masciocchi N and Pettinari R (2013). Mixed-ligand Cu (II) vanillin Schiff base complexes; effect of coligands on their DNA binding, DNA cleavage, SOD mimetic and anticancer activity. *Eur. J. Med. Chem.,* **60**: 216-232.

Tobriya SK (2014). Biological applications of Schiff Base and its metal complexes-A Review. *Int. J. Sci. Res.,* **3**(9): 1254-1256.

Touqeer S, Saeed MA, Adnan S, Mehmood F and Ch MA (2014). Antibacterial and antifungal activity of *Melaleuca decora* and *Syngonium podophyllum*. *R. J. P. T.,* **7**(7): 776-778.

Toxicity-Up AO (2001). OECD guideline for testing of chemicals. *O. E. C. D.: Paris, France*, pp.1-14.

Vashi K and Naik H (2004). Synthesis of novel Schiff base and azetidinone derivatives and their antibacterial activity. *J. Chem.,* **1**: 272-275.

Wiysonge CS, Bradley HA, Volmink J, Mayosi BM and Opie LH (2017). Beta-blockers for hypertension. *C. D. S. R.* (1).

Zhang N, Fan YH, Zhang Z, Zuo J, Zhang PF, Wang Q and Bi CF (2012). Syntheses, crystal structures and anticancer activities of three novel transition metal complexes with Schiff base derived from 2-acetylpyridine and l-tryptophan. *Inorg. Chem. Commun.,* **22**: 68-72.